Desalination and Water Treatment
www.deswater.com

doi:10.5004/dwt.2018.22199

111 (2018) 297–309
April

Biosorption of thallium(I) and cadmium(II) with the dried biomass of *Pestalotiopsis* sp. FW-JCCW: isotherm, kinetic, thermodynamic and mechanism

Kangning Chen[a], Huosheng Li[b,d,*], Lingjun Kong[a], Yan Peng[a], Diyun Chen[c], Jianrong Xia[a], Jianyou Long[a,*]

[a]*Guangzhou University, School of Environmental Science and Engineering, 510006, Guangzhou, China, email: kangningchan@gmail.com (K. Chen), kongl_jun@163.com (L. Kong), pengyann@126.com (Y. Peng), cdy@gzhu.edu.cn (D. Chen), xiajianrong@gzhu.edu.cn (J. Xia), Tel. +86 020 393 669 37, Fax +86 020 393 669 46, email: longjyou@gzhu.edu.cn (J. Long)*
[b]*Collaborative Innovation Center of Water Quality Safety and Protection in Pearl River Delta, Guangzhou University, Guangzhou 510006, China, Tel. +86 020 39366505, email: hilihuo@163.com (H. Li)*
[c]*Guangdong Provincial Key Laboratory of radionuclides pollution control and resources, Guangzhou 510006, China, email: cdy@gzhu.edu.cn (D. Chen)*
[d]*Key Laboratory for Water Quality and Conservation of Pearl River Delta, Ministry of Education and Guangdong Province, Guangzhou University, China*

Received 9 December 2017; Accepted 20 March 2018

ABSTRACT

In this study, the dried biomass of strain *Pestalotiopsis* sp. FW-JCCW was employed as an adsorbent for the biosorption of thallium (Tl) and cadmium (Cd). Influential factors including reaction pH, initial concentration of Tl^+ and Cd^{2+}, agitation speed, reaction temperature and contact time on the biosorption capacity of Tl^+ and Cd^{2+} were investigated. Isotherm tests showed that the Langmuir model provides the best fit for equilibrium data of both metals, with maximum biosorption capacity of 99.80 mg/g for Tl^+ and 98.01 mg/g for Cd^{2+}. In addition, the pseudo-second-order model described biosorption kinetics more effectively than the pseudo-first-order model. Thermodynamic parameters indicated that biosorption of Tl^+ and Cd^{2+} is a spontaneous and endothermic process. In addition, the biosorbent was characterized through Brunauer Emmett Teller analysis (BET), Fourier transform infrared spectroscopy (FTIR), scanning electron microscopy and energy disperse spectroscopy (SEM-EDS) and X-ray photoelectron spectroscopy (XPS). The characterization results demonstrate that functional groups (C-O, -OH or - NH, -CN and -COOH) on the surface of the strain contribute to the biosorption. In conclusion, *Pestalotiopsis* sp. FW-JCCW can be used as an effective biosorbent for removing Tl^+ and Cd^{2+} from wastewater.

Keywords: Pestalotiopsis sp.; FW-JCCW; Biosorption; Isotherms; Thallium; Cadmium

1. Introduction

With rapid global industrialization, the release of heavy metals into the environment is a considerable concern [1–3]. Heavy metals accumulation in the environment and associated human exposure can be detrimental, even at low concentrations [4,5]. Thallium (Tl) and Cadmium (Cd) are highly toxic metals that can endanger human health and ecosystem; they are often discharged into the environment without adequate treatment. Tl and its compounds are mainly leached from ore-processing sites and enter human body through the digestive system or skin contact, causing mutagenicity and carcinogenicity [6,7]. The Minimum Lethal Dose (MLD) of Tl for adults and children is 12 and 8.8 mg/kg, respectively [8]. Cd is mainly derived from metal refineries, waste batteries and paints, and can cause kidney damage or other diseases [9,10]. According to the *National Primary Drinking Water Regulations* of the United States Environmental Protection Agency, the Maximum Contaminant Level (MCL) of Tl and Cd in drinking water is 0.002 and 0.005 mg/L, respectively [11–13].

*Corresponding author.

Conventional physiochemical methods for heavy metal remediation include precipitation, filtration, coagulation evaporation, ion exchange, membrane separation and solvent extraction [14–16]. However, from the perspective of being cost-effective and sustainable, these methods are inefficient, but expensive, particularly at low metal concentrations of 1–100 mg/L [17]. Compared with these techniques, biosorption is a more economical and efficient for remedying heavy metal pollution. It is a physiochemical process in which a certain type of biomass spontaneously aggregates and binds contaminants to its cell structure [18]; it is considered a cost-effective biotechnology method for handling complex wastewater containing multiple metals [19]. Biosorption tests are typically performed using bacteria, fungi, and algae as biosorbents, because of their abundant mycelium, fungi tend to perform biosorption efficiently, suggesting that they have numerous biosorption sites, with enhanced biosorption performance [20]. Previous studies have indicated that many fungi species are proficient biosorbents for biological adsorption, with considerable biosorption performance. For example, Kwon et al. [21] reported effective lead and zinc biosorption with the extracellular polysaccharide of *Pestalotiopsis* sp. KCTC 8637P, indicating that *Pestalotiopsis* sp. is a potentially useful biosorbent for heavy metals removal. Thus, this fungal strain could be applied to the biosorption of other heavy metals such as Tl and Cd, and to the authors' knowledge, no such studies have yet been conducted.

In the present study, the dried biomass of the endophytic fungi *Pestalotiopsis* sp. FW-JCCW was employed to remove Tl^+ and Cd^{2+} from an aqueous solution. Batch experiments were performed to study the effect of reaction pH, initial concentration of both metals, agitation speed, reaction temperature and contact time on Tl^+ and Cd^{2+} removal. In addition, isotherm, kinetics and thermodynamic models were used to describe the biosorption process. Furthermore, the surface structure and functional groups were characterized through BET analysis, FTIR, SEM-EDS and XPS both before and after biosorption.

2. Materials and methods

2.1. Isolation of endophytic fungi resistant to Tl^+ and Cd^{2+}

The method used to isolate fungi is similar to that presented in the authors' previous study (Long et al.) [22]. In brief, the healthy roots and stems of *Miscanthus* were collected from Dabaoshan tailings in Shaoguan, Guangdong Province, China (N24°33′51.60″, E113°42′37.76″). The fresh plants were cut and divided into roots, stems and leaves after washing with tap water to remove soil and other attachments. The cut parts were surface-disinfected with 75% ethanol for 2 min and 5% sodium hypochlorite solution for 1 min, washed with sterile water three times to remove residual chemicals, and then further cut into 0.5 cm segments with sterile blades and cultured on Czapek's medium containing 20 mg/L Tl^+ and Cd^{2+} at 25°C for 48 h. The mature colonies grown in the culture media were transferred to a new media containing higher concentration of Tl^+ and Cd^{2+}. These steps were repeated for domestication with increasing concentrations of Tl^+ and Cd^{2+}, until the Minimum Inhibitory Concentration (MIC) of the fungal colony was obtained. The resulting strain showed excellent resistance to both Tl^+ and Cd^{2+} and was subjected to proliferation and culture to serve as an adsorbent for subsequent biosorption [23].

2.2. Chemicals and reagents

All reagents were of analytical grade, available from Guangzhou Huaxin reagent Co. Ltd. (Guangdong, China). The working solution was serially diluted from standard solution (1000 mg/L) daily. Deionized water was prepared using the DI water equipment YL05-20L 75G, (Shenzhen, China). Endophytic fungi were inoculated into a potato dextrose broth and cultured at 25°C in 250 ml triangle flasks on a shaker with an agitation speed of 150 rpm for 48 h. The fungal biomass collected through filtration was then thoroughly washed with deionized water to remove any remaining media, dried in an oven at 100°C for 2 h, and ground to a powder for use as an adsorbent in future biosorption.

2.3. Phylogenetic analysis of strain Pestalotiopsis sp. FW-JCCW

Pestalotiopsis sp. FW-JCCW 16S rDNA was extracted and amplified using polymerase chain reaction (PCR; ABI ProFlex 96-well). The following universal primers were designed: 5′-TCCGTAGGTGAACCTGCGG-3′ and 5′-TCCTCCG CTTATTGATATGC-3′. The amplification program was conducted as follows: pre-denaturation for 4 min at 94°C; 32 cycles of denaturation for 1 min at 94°C, annealing for 40 s at 55°C, extension for 40 s at 72°C; and final extension for 3 min at 72°C. Next, the resulting products were purified, sequenced, and analyzed on the MEGA5.2 to perform a multiple sequence alignment comparison with the GenBank database. The neighbor-joining phylogenetic tree was built with Kimura-2 model to analyze sequence similarities [24].

2.4. Batch experiments

Experimental factors were tested to determine the optimum biosorption conditions for Tl^+ and Cd^{2+} by using an adsorbents dosage of 2 g/L in a 100 ml solution. The experimental factors included reaction pH (2–9), initial concentrations of both metals (20–100 mg/L), agitation speed (60–210 rpm), reaction temperatures (20–40°C) and contact time (0–90 min). All batch experiments were repeated in triplicate, and the results were expressed in average value with standard deviation. The concentrations of Tl^+ and Cd^{2+} in the aqueous solution were measured by inductively coupled plasma atomic emission spectroscopy (ICP-AES) after centrifugation and wet digestion. The biosorption capacities (mg/g) of both Tl^+ and Cd^{2+} were evaluated using the following equation [25]:

$$q_e = \frac{(C_0 - C_e)V}{M} \tag{1}$$

where q_e is the equilibrium Tl^+ or Cd^{2+} biosorption capacity of the biosorbent (mg/g dry biomass); C_0 and C_e are the initial and residual metal concentration of Tl^+ and Cd^{2+} in solu-

tion, respectively (mg/L); V is the volume of the solution (L), and M is the mass of the biomass used (g dry biomass).

2.5. Isotherms

To understand the biosorption processes for Tl^+ and Cd^{2+} and estimate their biosorption characteristics, the fitting of the Langmuir and Freundlich model was examined [26]:

$$\frac{1}{q_e}=\frac{1}{q_{\max}K_L}\frac{1}{C_e}+\frac{1}{q_{\max}} \tag{2}$$

where q_{max} (mg/g) represents the maximum biosorption capacity of the monomolecular layer of the biosorbent and K_L (L/mg) is associated with the affinity of the binding sites [27]. In addition, the dimensionless separation factor, R_L is an essential coefficient of the Langmuir isotherm and is defined as:

$$R_L=\frac{1}{1+K_LC_O} \tag{3}$$

where C_0 is the initial concentration of metal ions in the solution (mg/L), R_L indicates the shape of the isotherm: when R_L>1, it is unfavorable; when R_L=1, it is linear; when 0<R_L<1, it is favorable; and when R_L=0, it is irreversible [28].

The Freundlich isotherm is generally expressed as follows:

$$q_e=K_FC_e^{1/n} \tag{4}$$

It can be rewritten linearly as follows:

$$lnq_e=\frac{1}{n}lnC_e+lnK_F \tag{5}$$

where K_F (L/g) is related to the biosorption capacity, and n is an empirical parameter related to the biosorption intensity.

2.6. Kinetics

The pseudo-first-order and pseudo-second-order models are the most frequently used models for describing the biosorption process; they are used to describe the biosorption of Tl^+ and Cd^{2+} [Eqs. (6) and (7)] [29] as follows:

$$\log\left(q_e-q_t\right)=\log q_e-\frac{k_1t}{2.303} \tag{6}$$

where q_e (mg/g) is the biosorption capacity at equilibrium, q_t (mg/g) is the quantity absorbed at time t, and k_1 (h^{-1}) is the rate constant at equilibrium.

The pseudo-second-order model, derived from the basis of solid phase sorption. It is used to describe the whole biosorption process and can be expressed by the following linear equation [30]:

$$\frac{t}{q_t}=\frac{1}{k_2q_e^2}+\frac{t}{q_e} \tag{7}$$

where q_e (mg/g) is the quantity of biosorption at equilibrium, q_t (mg/g) is the quantity of biosorption at time t (h^{-1}), and k_2 (g/mg/h) is the rate constant of the biosorption process.

2.7. Thermodynamics

Thermodynamic parameters are also significant factors for the biosorption of heavy metals. The parameters of Gibbs free energy (ΔG^0), enthalpy (ΔH^0) and entropy (ΔS^0) were used to describe the thermodynamic behavior for Tl^+ and Cd^{2+} during biosorption of *Pestalotiopsis* sp. FW-JCCW at three temperatures (293, 303, and 313 K), in the following equations [31]:

$$k_d=\frac{C_0-C_e}{C_e}\frac{V}{M} \tag{8}$$

$$ln\,k_d\frac{\Delta S^0}{R}-\frac{\Delta H^0}{RT} \tag{9}$$

$$\Delta G^0=\Delta H^0-T\Delta S^0 \tag{10}$$

2.8. Characterization of the dried biomass

2.8.1. Brunauer Emmett Teller (BET) analysis

The specific surface area and pore size distribution of *Pestalotiopsis* sp. FW-JCCW were determined using nitrogen adsorption at 77 K on a TriStarII 3020 Series Surface Area and Porosity Analyzer (Micromeritics Instrument Corporation, USA) [32].

2.8.2. Fourier transform infrared spectroscopy (FTIR) analysis

Both before and after biosorption, the dried biomass was mixed and pulverized with KBr, pressed into a uniform transparent sheet, and finally placed in a BRUKER TENSOR27 Raman infrared spectrometer to measure the functional groups at a wavenumber range of 4000–400 cm^{-1} [33].

2.8.3. Scanning electron microscopy and energy disperse spectroscopy (SEM-EDS) analysis

The morphology and elementary compositions of dried biomass both before and after biosorption were determined by SEM-EDS (JSM-7001F) at room temperature.

2.8.4. X-ray photoelectron spectroscopy (XPS) analysis

The XPS spectra of the biosorbents before and after biosorption were obtained using a Theta Probe Angle-Resolved XPS System (hv=1486.6 eV; Kratos Axis Ultra, Japan) to identify the element and compounds of *Pestalotiopsis* sp. FW-JCCW. Correction of the deviation of the binding energy (BE) owing to relative surface charging was conducted at the the C 1s level, with BE of 284.6 eV as an inter-

nal standard. All XPS spectra were fitted using XPSPEAK4.1 [34,35].

2.9. Desorption studies

To understand the feasibility and efficiency of using this adsorbent in recycling, desorption of Tl^+ and Cd^{2+} onto the strain *Pestalotiopsis* sp. FW-JCCW was performed at a pH of 5 and 6 for Tl^+ and Cd^{2+}, respectively. Adsorption-desorption cycles were repeated four times with 0.1 mol/L HCl at room temperature. Before biosorption, 0.01 g of the biosorbents of Tl^+ and Cd^{2+} were added to 10 ml of the eluate in a 50 ml Erlenmeyer flasks and continuously stirred at 150 r/min for 60 min. The final concentrations of Tl^+ and Cd^{2+} in the supernatant were determined through ICP-AES individually, and the desorption efficiency was calculated using the following formula [36].

$$\text{Desorption efficiency}(\%) = \frac{\text{Amount of Tl/Cd desorbed}}{\text{Amount of Tl/Cd Absorbed}} \times 100\%$$

3. Results and discussion

3.1. Phylogentic analysis of strain Pestalotiopsis sp. FW-JCCW

The phylogenetic tree for the ITS gene sequence of this fungi strain is shown in Fig. 1, blasted with other ITS genetic sequences from the GenBank. The strain has more than 98% sequence homology with *Pestalotiopsis* sp., suggesting that the isolated strain can be identified as *Pestalotiopsis* sp. FW-JCCW (accession number: KX349438).

Few studies on heavy metals biosorption by *Pestalotiopsis* sp. have been reported. However, Ramrakhiani et al. [37] reported the feasibility of this fungal strain in removing Pb^{2+} and Zn^{2+} in wastewater and indicated that it is a potential biosorbent capturing other heavy metals such as Tl^+ and Cd^{2+}.

3.2. Influencing factors on Tl^+ and Cd^{2+} removal

The reaction pH is crucial in the biosorption of heavy metals, because it affects the interaction of biosorbents and heavy metal ions in aqueous solution [38,39]. Fig. 2a shows that the reaction pH has a significant effect on the biosorption of the two metals. At low pH, the biosorption efficiencies of Tl^+ and Cd^{2+} increases with an increase in the reaction pH; a maximum efficiency was reached at pH 5 and 6 for Tl^+ and Cd^{2+}, respectively. The biosorption capacity of Tl^+ increases from 12.21 to 20.06 mg/g when the pH increases from 2 to 5. Similarly, the biosorption capacity of Cd^{2+} increases from 10.90 to 25.17 mg/g when the pH increased from 2 to 6. These changes occurred because low pH creates a competitive relationship among H_3O^+, Tl^+, and Cd^{2+}, causing the protonation of active sites and resulting in low biosorption [40]. As the pH gradually increases, a greater number of negatively charged surfaces became available for ion-exchange of Tl^+ and Cd^{2+}, leading to an increase in biosorption. However, the continual in pH leads to an increase in negatively charged hydroxide ions in the solution, which compete with the active sites on the biosorbent surface and react with metal ions to form precipitates, resulting in a decrease in the biosorption capacity [41,42].

Similar trends in the removal of the two metals were noted over an initial concentration range of 20–100 mg/L (Fig. 2b). The biosorption capacity of Tl^+ increased from 12.16 to 44.18 mg/g, whereas that of Cd^{2+} increased from 10.25 to 36.05 mg/g, because the initial concentration generated an crucial driving force for overcoming mass transfer resistance of metals between the aqueous and solid phases. Hence, more metals could be captured onto the active sites on the surface of the strain. Similar results were reported by Kim et al. [43].

As shown in Fig. 2c, the biosorption capacity of both metals increases with the agitation speed, it reached a maximum at 150 r/min with 22.69 mg/g for Tl^+ and 27.86 mg/g for Cd^{2+}, and then gradually decreased. In this biosorption

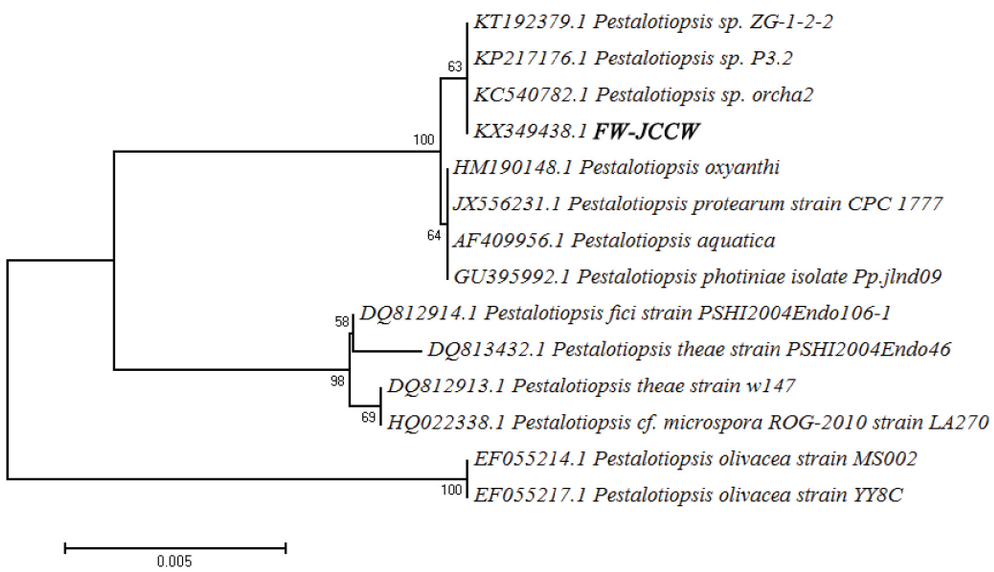

Fig. 1. The phylogenetic tree of *Pestalotiopsis* sp. and related strains with the neighbor-joining method.

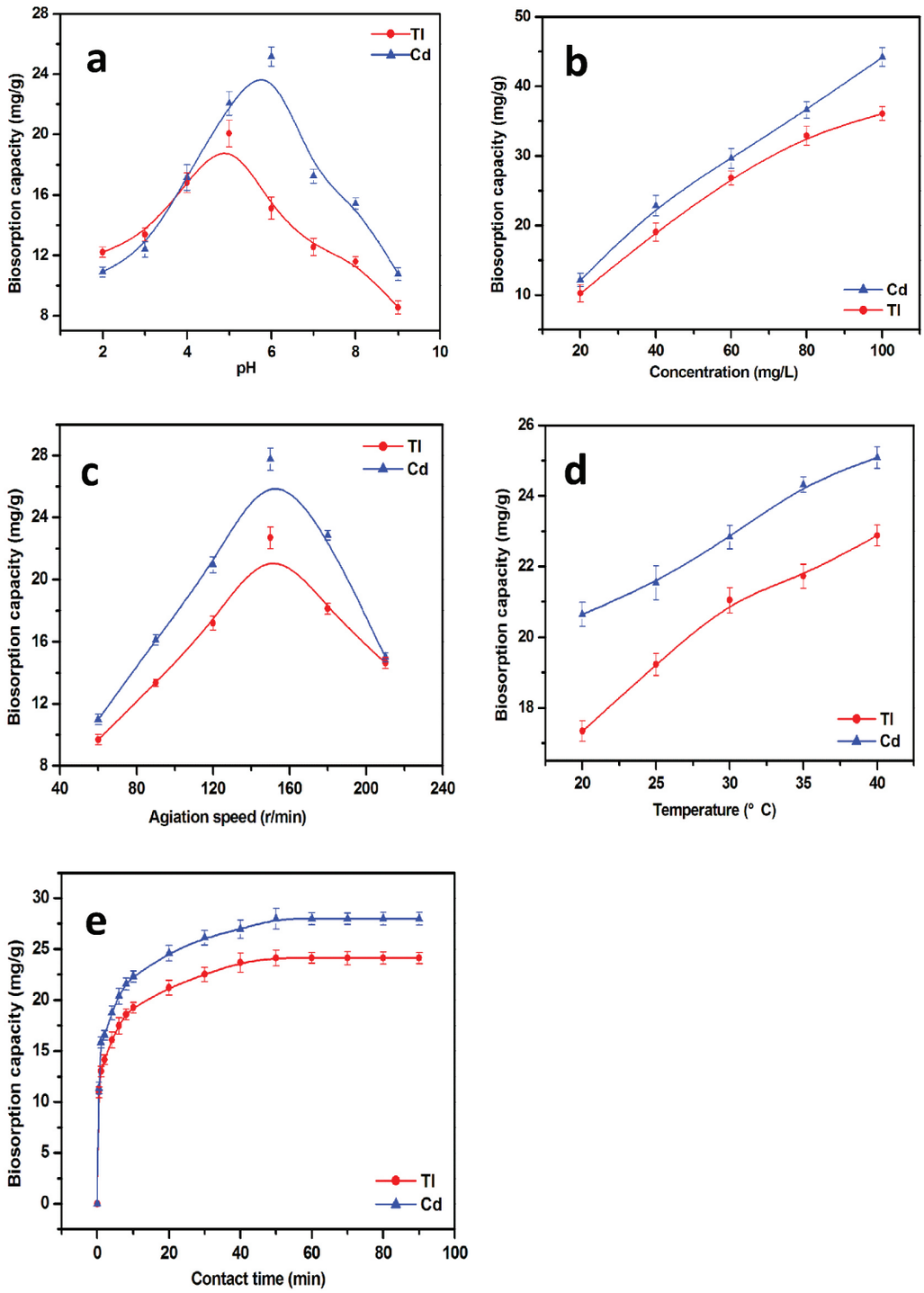

Fig. 2. Effects of different environmental parameters on the biosorption of Tl^{+} and Cd^{2+} by *Pestalotiopsis* sp. FW-JCCW (a) pH, (b) Tl^{+} and Cd^{2+} initial concentration, (c) agitation speed, (d) temperatures and (e) contact time.

system, the higher agitation speed provided more opportunities for contact between the metal ions and the biosorbent binding sites, which promoted the biosorption capacity. However, the decline in biosorption at higher speed may be due to improper contact between the metal ions and the binding sites with respect to the vortex formation, making Tl^{+} and Cd^{2+} biosorption less effective. Similar results have been reported with the removal of other heavy metals [44].

The biosorption capacity progressively increased with increase in the reaction temperature (Fig. 2d), suggesting that Tl^+ and Cd^{2+} have an endothermic nature during the biosorption process because of three possible reasons: (1) the increased temperature increases the diffusion rate of Tl^+ and Cd^{2+} to the biosorbent; (2) the increased temperature increases the degree of ionization of functional groups, which is more conducive to biosorption; and (3) the high temperature is more favorable for metal and biosorbent complex formation [45]. Similar phenomena were reported by Badawia et al. [46] with the biosorption of Al^{3+} and Pb^{2+} onto the biomass of chitosan-tannic acid-modified biopolymers.

The biosorption of Tl^+ and Cd^{2+} on the dried biomass comprised two phases of biosorption: a primary fast phase and a slow phase (Fig. 2e). In the fast phase (< 10 min), the initial rate of biosorption for both metals was fast, which is potentially attributed to the presence of numerous active sites on the surface of the biosorbent, available for Tl^+ and Cd^{2+} at a initial high concentration gradient. In the slow phase, the biosorption capacity increased slowly with time (from 10 to 50 min); this is related to few available active sites and low concentration gradient during this period, resulting in a reduction in effective collisions between active sites and metal ions [47]. Taken together, the results indicate that the biosorption of *Pestalotiopsis* sp. FW-JCCW to Tl^+ and Cd^{2+} is a rapid process.

3.3. Isotherms

Table 1 and Fig. 3 (a, b) summarize the linear fitting of experimental data with Langmuir and Freundlich models. The correlation coefficients of both metals with the Langmuir model Fig. 3a (Tl: 0.9980, Cd: 0.9990) were higher than those with the Freundlich model Fig. 3b (Tl: 0.9939, Cd: 0.9888), suggesting that the Langmuir model is more favorable for describing the biosorption process occurring with Tl^+ and Cd^{2+}. Table 2 shows the results of other research work with respect to Tl^+ and Cd^{2+} biosorption for several microbes used as adsorbents. In this study, the maximum biosorption capacities were 99.80 and 98.01 mg/g for Tl^+ and Cd^{2+}, respectively. The results agree with those of a study using the dried biomass of *Landoltia punctata* and *Spirodela polyrhiza,* for which the maximum Pb^{2+} adsorption capacity were 250 and 200 mg/g, respectively [48].

3.4. Kinetics

Dynamics curve fittings for the biosorption of Tl^+ and Cd^{2+} are presented in Figs. 4a, b, and the corresponding correlation parameters for each model are listed in Table 3. For the two metals, the correlation coefficients obtained by fitting the experimental data of the pseudo-second-order model Fig. 4a (Tl: 0.9990, Cd: 0.9995) were higher than those for the pseudo-first-order model Fig. 4b (Tl: 0.9919, Cd: 0.9883), suggesting that the pseudo-second-order model is more suitable for explaining the biosorption kinetics of Tl^+ and Cd^{2+}. Next, the q_e values calculated by the pseudo-second-order model (Tl: 12.72 mg/g, Cd: 11.33 mg/g) were found to be approximately equal to the corresponding experimental values (Tl: 12.45 mg/g, Cd: 10.89 mg/g), however, the q_e values of the pseudo-first-order model (Tl: 5.64 mg/g, Cd: 6.64 mg/g) were only equal to approximately 50% of the values. Thus, the pseudo-second-order

Table 1
Constants simulated by Langmuir and Freundlich models for the biosorption of Tl^+ and Cd^{2+} by *Pestalotiopsis* sp. FW-JCCW

Biosorbate	Langmuir model			Freundlich model			
	K_L	q_{max} (mg/g)	R^2	R_L	n	K_F	R^2
Tl	0.0092	99.80	0.9980	0.5205	1.3421	1.6616	0.9939
Cd	0.0073	98.01	0.9990	0.5776	1.3067	1.2869	0.9888

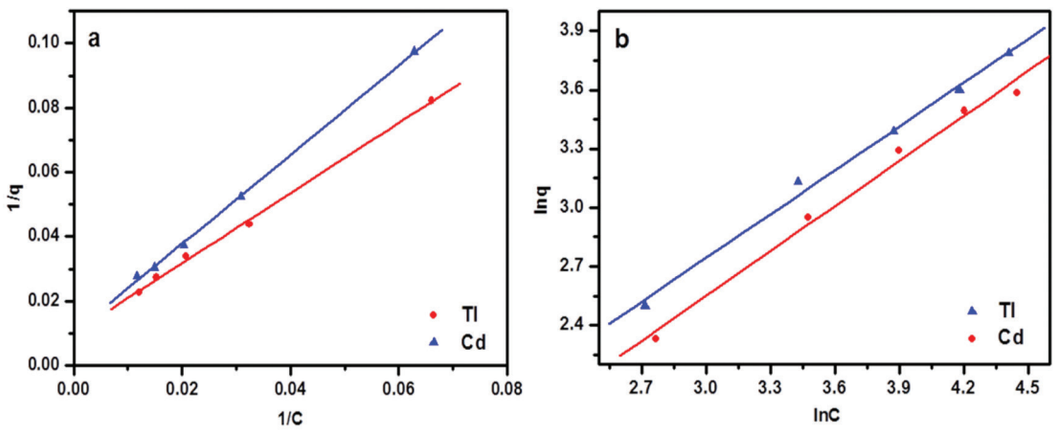

Fig. 3. Plots of isotherms of Tl^+ and Cd^{2+} biosorption on *Pestalotiopsis* sp. FW-JCCW. Langmuir (a) and Freundlich (b) models.

Table 2
Comparison of biosorption capacity with other biosorbents

Biomass type	Metal	q_{max} (mg/g)	Reference
Modified *Aspergillus niger*	Tl	0.97	[9]
Pseudomonas fluorescens	Tl	93.76	[8]
Scenedesmus acuminutus	Tl	833.33	[13]
Pestalotiopsis sp.	Tl	99.8	this study
Aspergillus niger	Cd	1.31	[19]
Penicillium chrysogenum	Cd	21.5	[16]
Penicillium purpurogenum	Cd	110.4	[20]
Pestalotiopsis sp.	Cd	98.01	this study

model is relatively more suitable for describing the kinetics of the *Pestalotiopsis* sp. FW-JCCW for the Tl and Cd biosorption processes.

3.5. Thermodynamics

The calculated thermodynamic parameters are presented in Table 4. The negative values of ΔG at all tested temperatures (293, 303, and 313K) indicated the spontaneity of Tl^+ and Cd^{2+} bioisorption by the dried biomass of *Pestalotiopsis* sp. FW-JCCW. The ΔG value decreased with increase in temperature, indicating that the biosorption is favorable at a higher temperature [49]; these results are similar to those of Henriques and B. Henriques [50]. The positive ΔH values indicated that the biosorption process of Tl^+ and Cd^{2+} on the surface of the dried biomass is inherently endothermic, and the positive values of ΔS imply an increase in randomness after biosorption.

3.6. Tl^+ and Cd^{2+} desorption

In practical applications, recycling after biological adsorption is crucial. As shown in Fig. 5, the desorption efficiencies of Tl and Cd onto *Pestalotiopsis* sp. FW-JCCW decreased by 7.27% and 10.60%, respectively, after four cycles, similar to the biosorption of lead ions from aqueous solution by *Sargassum filipendula* reported by Ayushi Verma [51].

3.7. *Characterization of* Pestalotiopsis *sp. strain*

3.7.1. FT-IR analysis

The FT-IR spectra before biosorption showed strong and broad bonds at 3399.61 cm^{-1}, indicating the bonded

Table 3
Constants simulated by the pseudo-first-order and pseudo-second-order model for the biosorption of Tl^+ and Cd^{2+} by *Pestalotiopsis* sp. FW-JCCW

Biosorbate	Experimental q_e (mg/g)	Pseudo-first-order			Pseudo-second-order		
		q_e (mg/g)	k_1 (min^{-1})	R^2	q_e (mg/g)	k_2 (g mg^{-1} min^{-1})	R^2
Tl	12.4450	5.6390	0.0550	0.9919	12.7227	0.0330	0.9990
Cd	10.8978	6.6359	0.1011	0.9883	11.3250	0.0324	0.9995

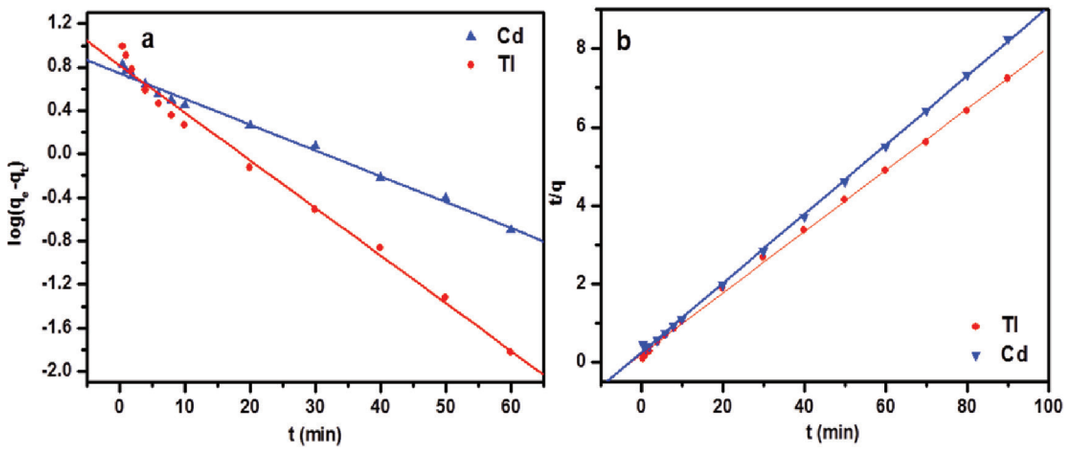

Fig. 4. Plots of isotherms of Tl^+ and Cd^{2+} biosorption on *Pestalotiopsis* sp. FW-JCCW. Pseudo-first-order (a) and pseudo-second-order (b) models.

Table 4
The thermodynamic parameters of *Pestalotiopsis* sp. FW-JCCW after biosorption of Tl^+ and Cd^{2+}

T(*K*)	Tl			Cd		
	Δ*G*(kJ/mol)	Δ*H*°(kJ/mol)	Δ*S*°(J/mol K)	Δ*G*(kJ/mol)	Δ*H*°(kJ/mol)	Δ*S*°(J/mol K)
293	–215.99			–174.56		
303	–388.33	128.87	17.24	–313.75	104.15	13.93
313	–560.73			–453.05		

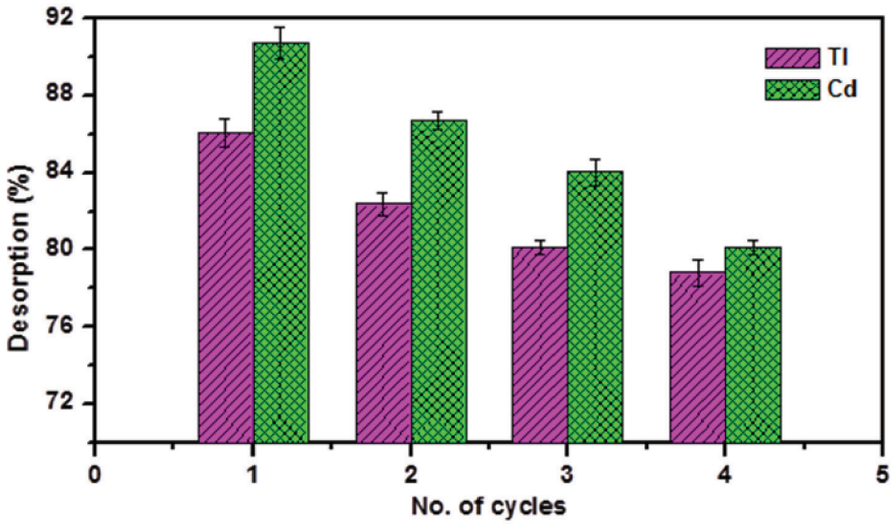

Fig. 5. Desorption efficiency and cycles for Tl^+ and Cd^{2+} biosorption by *Pestalotiopsis* sp. FW-JCCW.

hydroxyl (-OH) or amine (-NH) groups (Fig. 6). After biosorption, the peak at 3399.61 cm^{-1} blue-shifted to 3419.86 cm^{-1} for Tl^+ and to 3458.79 cm^{-1} for Cd^{2+}, respectively, indicating that the two groups had participated in biosorption [52,53]. The peak of the N-H group (because of the bending of amide or C-N stretching in -CO-NH- at 1617.13 cm^{-1}) blue-shifted to 1637.38 cm^{-1} for Tl^+ and to 1656.85 cm^{-1} for Cd^{2+}, respectively, indicating that these functional groups are associated with Tl and Cd biosorption processes. Another peak at 1043.22 cm^{-1} shows that C-OH stretching blue-shifted to 1052.56 cm^{-1} and 1062.69 cm^{-1} for Tl^+ and Cd^{2+}, respectively, indicating that C-OH is also involved in the biosorption of Tl^+ and Cd^{2+} [54].

3.7.2. SEM-EDS analysis

The surface of the biosorbent was regular and homogeneously smooth prior to biosorption (Fig. 7). The specific surface area and pore size distribution of *Pestalotiopsis* sp. FW-JCCW were 17.23 m^2 g^{-1}, and 0.0034 cm^3 g^{-1}, respectively. However, numerous pores of varied sizes, along with scale-like precipitates, were observed on the surface of the dried biomass after biosorption, which may be attributed to the adsorbed metal Tl and Cd causing the

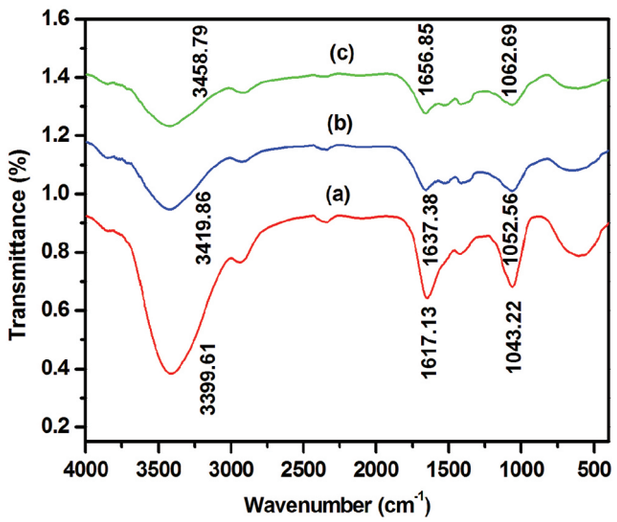

Fig. 6. FT-IR spectrum of *Pestalotiopsis* sp. FW-JCCW before and after biosorption, (a) before biosorption, (b) after Tl^+ biosorption, and (c) after Cd^{2+} biosorption.

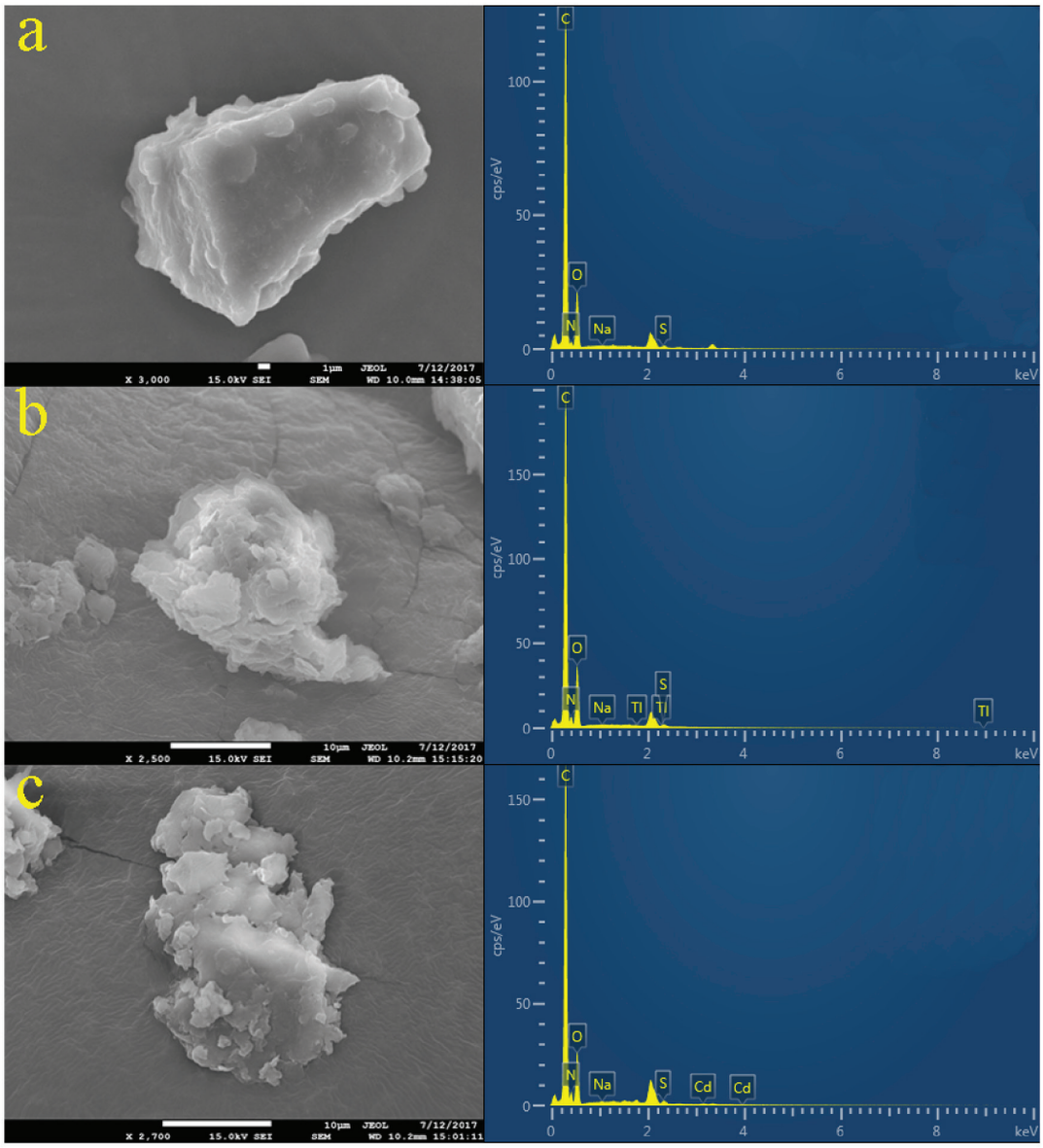

Fig. 7. SEM-EDS analysis of *Pestalotiopsis* sp. FW-JCCW. Before (a), Tl^{+} biosorption (b), and Cd^{2+} biosorption (c).

uneven biosorbent surface [55]. In addition, according to the EDS analysis, Tl and Cd peaks appeared on the EDS spectra after biosorption of Tl^{+} and Cd^{2+}, whereas no such peaks were found in the spectra before biosorption. This result confirms that the morphological changes were due to the presence of the two heavy metals [56]. Simultaneously, changes in the carbon, oxygen and nitrogen contents after biosorption (Table 5) suggest that surface functional groups of the biosorbent are involved in the reaction. This finding is similar to the result reported by Kulkarni et al. [57], who used *Bacillus laterosporus* to adsorb Cd^{2+} and Ni^{2+} from industrial wastewater.

3.7.3. XPS analysis

The XPS results (Fig. 8) indicated that after Tl^{+} and Cd^{2+} biosorption, a new peak appeared with a BE of 113.2 eV for Tl^{+} and 402.4 eV for Cd^{2+}[58], which belonged to the Tl 4f and Cd 3d core levels, respectively. Hence, Tl^{+} and Cd^{2+} were successfully absorbed onto the surface of the dried biomass.

The C1s peaks were split into the following sub-peaks: C-H at around 285 eV, C-O and C-N at around 286 eV, and O=C-O and C=O at around 288 eV (Table 6, Figs. 9a, d, g) [59]. After biosorption, the ratio of the peak area of C-C/C-H increased from 61.49% to 68.96% for Tl^{+} and 80.42%

Table 5
EDS analysis of *Pestalotiopsis* sp. FW-JCCW before and after Tl^+ and Cd^{2+} biosorption

FW-JCCW	Wt%						
	C	O	N	S	Na	Tl	Cd
Before biosorption	67.59	29.14	3.21	0.04	0.02	0	0
Tl-loaded	73.38	21.86	4.12	0.27	0.03	0.28	0
Cd-loaded	75.35	19.51	3.03	0.53	0.08	0	1.46
FW-JCCW	At%						
	C	O	N	S	Na	Tl	Cd
Before biosorption	73.38	23.51	2.25	0.08	0.03	0	0
Tl-loaded	78.47	17.55	3.64	0.11	0.02	0.02	0
Cd-loaded	81.09	16.08	2.38	0.21	0.04	0	0.17

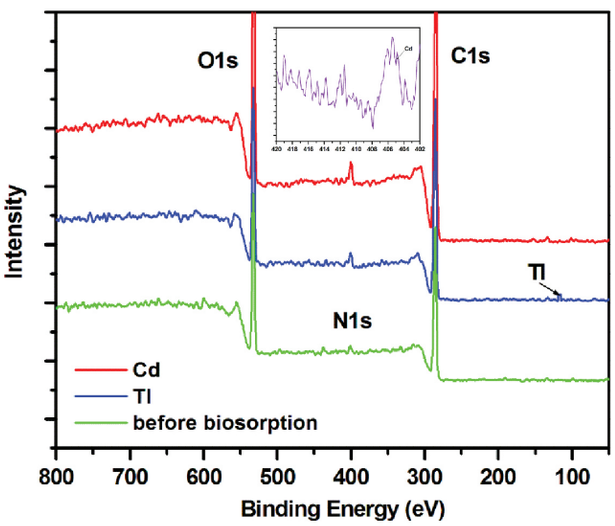

Fig. 8. The full XPS analysis of *Pestalotiopsis* sp. FW-JCCW before and after Tl^+ and Cd^{2+} biosorption.

for Cd^{2+}, respectively, that of C-O/C-N decreased from 36.86% to 28.29% and 16.64 for Tl^+ and Cd^{2+}, respectively; and the contents of O=C-O/C=O increased from 1.65% to 2.75% and 2.94% for Tl^+ and Cd^{2+}, respectively, which may be due to Tl^+ and Cd^{2+} biosorption and surface changes of the biosorbent loaded with Tl and Cd. The results show that the functional groups such as carboxyl, hydroxyl, alcohol, ketone and ether may also be involved in the biosorption of thallium and cadmium. The N 1s XPS spectra of the Tl^+ and Cd^{2+} loaded biosorbent were split into three individual component peaks as follow: R-NH_2/R_2-NH at around 400 eV; R-NH_3^+ at around 402 eV; and NO_2^- at around 406 eV (Figs. 9b, e, h) [60]. After biosorption, the amount of R-NH_2/R_2-NH increased from 68.18% to 77.80% for Tl^+, but decreased to 62.92% for Cd^{2+}; and the amount of R-NH_3^+ decreased from 31.82% to 22.20% for Tl^+ and to 23.93% for Cd^{2+}, indicating that R-NH_2/R_2-NH and R-NH_3^+ may be involved in the biosorption. Similarly, the O 1s XPS spectra were split into four component peaks: O-H at around 531 eV, C=O at around 531.5 eV, and C-O at around 532.65 eV (Figs. 9c, f, i). A new peak (C-OH) appeared at 534 eV with a percentage of 1.87% for Tl^+ and 6.60% for Cd^{2+}, which is attributed to the emergence of Tl-O/Cd-O with the original oxygen-containing functional groups peaks (C-O/C=O) on the surface of *Pestalotiopsis* sp.. After biosorption, the peak area percentage of C-O decreased from 87.43% to 77.13% for Tl^+ and 83.10% for Cd^{2+}, whereas that of C=O decreased from 12.57% to 8.52% for Tl^+ and 6.49 % for Cd^{2+}. This result is similar to that presented in the previous study of W. Zhang [61].

4. Conclusions

The dried biomass of *Pestalotiopsis* sp. FW-JCCW potentially acts as a highly effective biosorbent for the removal of Tl^+ and Cd^{2+} from wastewater. In addition, the reaction pH, initial concentration, reaction temperature, agitation speed and contact time have substantial influence on the biosorption of both Tl^+ and Cd^{2+}. For Tl^+, the maximum biosorption capacity reaches 99.80 mg/g at a reaction pH of 5.0, initial concentration of 100 mg/L, agitation speed of 150 rpm, temperature of 313 K and contact time of 50 min, with a biological biosorption dose of 2 g/L in 100 ml. For Cd^{2+}, the maximum biosorption capacity reaches 98.01 mg/g at pH of 6.0, initial concentration of 100 mg/L, agitation speed at 150 rpm, temperature of 313 K with a contact time of 50 min.

The Langmuir isotherm model proficiently describes the biosorption of Tl^+ and Cd^{2+}. In addition, the pseudo-second-order kinetic model performs more effectively describes biosorption kinetics than the pseudo-first-order model. Thermodynamic analyses indicate that a spontaneous and endothermic biosorption process occurs. Furthermore, characterization by BET analysis, FTIR, SEM-EDS and XPS demonstrate that various functional groups (C-O,

Table 6
Summary of binding energies for the biosorbents

	E_B(eV)	Possible group	Original (%)	Tl-FW-JCCW (%)	Cd-FW-JCCW (%)
C 1s	284.78	C-C/C-H	61.49	68.96	80.42
	286.08	C-O/C-N	36.86	28.29	16.64
	287.78	C=O/O=C-O	1.65	2.75	2.94
	288.00	O=C-OH/O=C-OR			
N 1s	399.88	R-NH_2/R_2-NH	68.18	77.80	62.92
	401.78	R-NH_3^+	31.82	22.20	23.93
	405.78	NO_2^-			13.16
O 1s	532.65	C-O	87.43	77.13	83.10
	531.50	O=C	12.57	8.52	6.49
	531.10	O-H		12.49	3.82
	533.90	C-OH		1.87	6.60

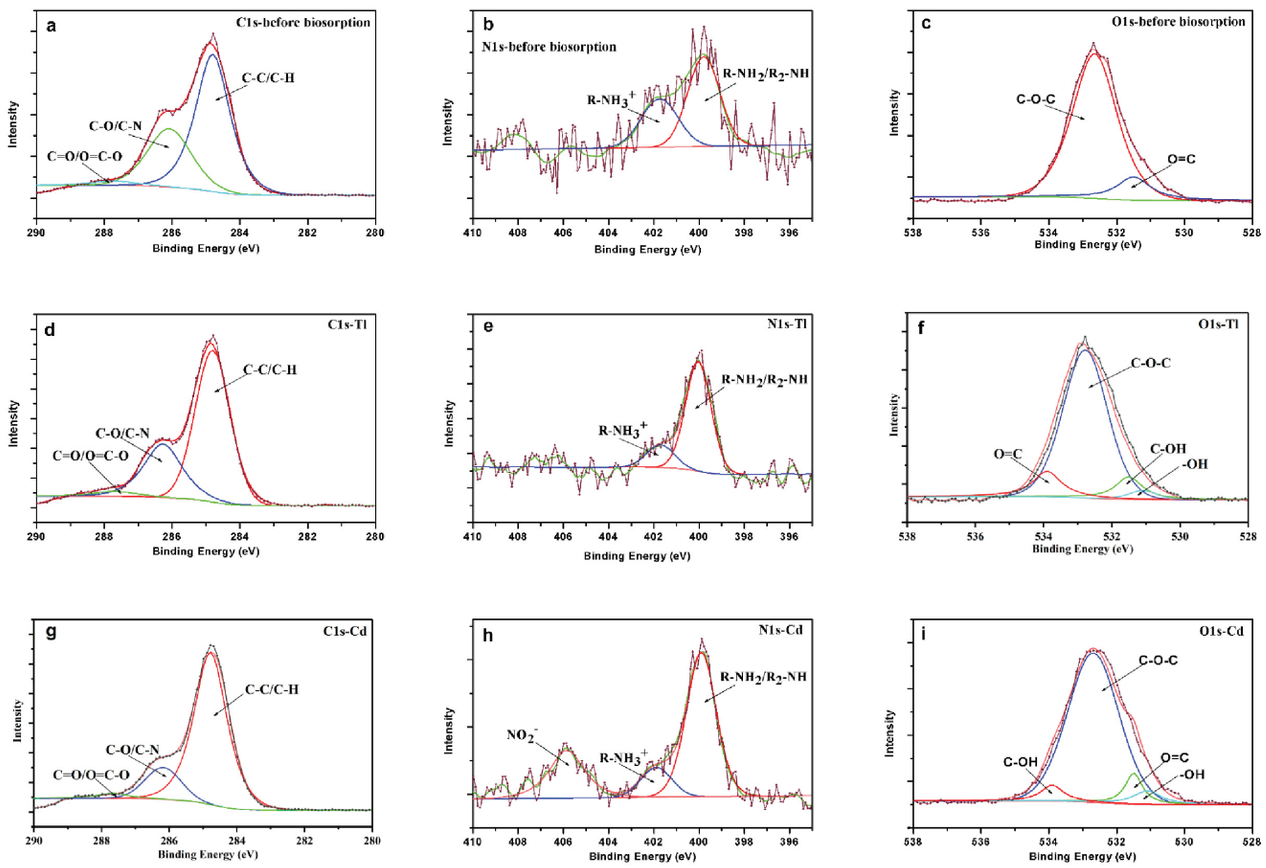

Fig. 9. The XPS analysis of C1s (a: C1s-before biosorption; d: C1s-Tl; g: C1s-Cd), N1s (b: N1s-before biosorption; e: N1s-Tl; h: N1s-Cd) and O1s (c: O1s-before biosorption; f: O1s-Tl; i: O1s-Cd) *Pestalotiopsis* sp. FW-JCCW before and after Tl^+ and Cd^{2+} biosorption.

-NH, -OH and -COOH) on the surface of the strain are involved in biosorption.

Acknowledgments

We gratefully acknowledge the financial support provided by National Natural Science Foundation of China (U1501231), Guangdong Innovation Platform Characteristic Innovation Project (2016KTSCX106), Guangzhou City Science and Technology Project (201804010281), Project of the Education Bureau of Guangzhou City (1201620219) and the High-level University Construction Project (Regional Water Environment Safety and Ecological Water Protection).

References

[1] A.A. Alqadami, M. Naushad, M.A. Abdalla, T. Ahamad, A.Z. Abdullah, S.M. Alshehri, A.A. Ghfar, Efficient removal of toxic metal ions from wastewater using a recyclable nanocomposite: A study of adsorption parameters and interaction mechanism, J. Clean. Prod., 156 (2017) 426–436.

[2] A.A. Alqadami, M. Naushad, Z.A. Alothman, A.A. Ghfar, Novel metal–organic framework (MOF) based composite material for the sequestration of U(VI) and Th(IV) metal ions from aqueous environment, ACS. Appl. Mater. Inter., 9 (2017) 36026–36037.

[3] M. Naushad, T. Ahamad, B.M. Al-Maswari, A. Abdullah, Nickel ferrite bearing nitrogen-doped mesoporous carbon as efficient adsorbent for the removal of highly toxic metal ion from aqueous medium, Chem. Eng. J., 330 (2017) 1351–1360.

[4] Z.A. AlOthman, M.M. Alam, M. Naushad, Heavy toxic metal ion exchange kinetics: Validation of ion exchange process on composite cation exchanger nylon 6,6 Zr (IV) phosphate, J. Ind. Eng. Chem., 19 (2013) 956–960.

[5] M. Naushad, Z.A. AL-Othman, M. Islam, Adsorption of cadmium ion using a new composite cation-exchanger polyaniline Sn (IV) silicate: Kinetics, thermodynamic and isotherm studies, J. Sol. Sci. Tech., 10 (2013) 567–578.

[6] A. Celik Demirbas, Removal of heavy metal ions from aqueous solutions via adsorption onto modified lignin from pulping wastes, Energy Sources, 27 (2005) 1167–1177.

[7] A. Demirbas, Heavy metal adsorption onto agro-based waste materials: A review, J. Hazard Mater., 157 (2008) 220–229.

[8] J.Y. Long, D.Y. Chen, J.R. Xia, D.G. Luo, B.F. Zheng, Y.H. Chen, Equilibrium and kinetics studies on biosorption of thallium (I) by dead biomass of *Pseudomonas fluorescens*, Pol. J. Environ. Stud., 26 (2017) 1591–1598.

[9] A.L. John Peter, T. Viraraghavan, Removal of thallium from aqueous solutions by modified *Aspergillus niger* biomass, Bioresour. Technol., 99 (2008) 618–625.

[10] Z.S. Birungi, E.M.N. Chirwa, The adsorption potential and recovery of thallium using green micro-algae from eutrophic water sources, J. Hazard. Mater., 299 (2015) 67–77.

[11] F. Costa, T. Tavares, Bioremoval of Ni and Cd in the presence of diethyl ketone by fungi and by bacteria – A comparative study, Int. Biodeterior. Biodegrad., 120 (2017) 115–123.

[12] S. Yapicia, H. Eroglub, Batch biosorption of radioactive thallium on solid waste of oleum rosea process. J. Chem. Technol. Biotechnol., 88 (2013) 2082–2090.

[13] S.B. Zainab, M.N.C. Evans, Bioreduction of thallium and cadmium toxicity from industrial wastewater using microalgae, Chem. Eng. Trans., 57 (2017) 1183–1188.

[14] X.Z. Li, Y.J. Wang, Y.S. Pan, H. Yu, X.L. Zhang, Y.P. Shen, S. Jiao, K. Wu, G.X. La, Y. Yuan, S.M. Zhang, Mechanisms of Cd and Cr removal and tolerance by macrofungus Pleurotus ostreatus HAU-2, J. Hazard. Mater., 330 (2017) 1–8.

[15] T. Vincent, J.M. Taulemesse, A. Dauvergne, T. Chanut, F. Testaa, E. Guibal, Thallium (I) sorption using Prussian blue immobilized in alginate capsules, Carbohydr. Polym., 99 (2014) 517–526.

[16] T. Skowronski, J. Pirszel, S.B. Pawlik, Heavy metal removal by the waste biomass of *Penicillium chrysogenum*, Water Qual. Res. J. Can., 36 (2001) 793–803.

[17] C. Pang, Y.H. Liu, X.H. Cao, M. Li, G.L. Huang, R. Hua, C.X. Wang, Y.T. Liu, X.F. An, Biosorption of uranium (VI) from aqueous solution by dead fungal biomass of *Penicillium citrinum*, Chem. Eng. J., 170 (2011) 1–6.

[18] H.P. Yuan, J.H. Zhang, Z.M. Lu, H. Min, C. Wu, Studies on biosorption equilibrium and kinetics of Cd^{2+} by *Streptomyces* sp. K33 and HL-12, J. Hazard. Mater., 164 (2009) 423–431.

[19] A. Kapoor, T. Viraraghavan, D.R Cullimore, Removal of heavy metals using the fungus *Aspergillus niger*, Biores. Technol., 70 (1999) 95–104.

[20] R. Say, N. Yilmaz, A. Denizli, Biosorption of cadmium, lead, mercury, and arsenic ions by the fungus *Penicillium purpurogenum*, Sep. Sci. Technol., 38 (2003) 2039–2053.

[21] G.S. Kwon, S.H. Moon, S.D. Hong, H.M. Lee, H.S. Kim, H.M. Oh, B.D. Yoon, A novel flocculant biopolymer produced by *Pestalotiopsis* sp. KCTC 8637P, Biotechnol. Lett., 18 (1996) 1459–1464.

[22] J.Y. Long, H.S. Li, D.Q. Jiang, D.G. Luo, Y.H. Chen, J.R. Xia, D.Y. Chen, Biosorption of strontium (II) from aqueous solutions by *Bacillus cereus* isolated from strontium hyperaccumulator *Andropogon gayanus*, Process Saf. Environ., 111 (2017) 23–30.

[23] C.S. Zhao, J. Liu, X.Y. Li, F.Z. Li, H. Tu, Q. Sun, J.L. Liao, J.J. Yang, Y.Y. Yang, N. Liu, Biosorption and bioaccumulation behavior of uranium on Bacillus sp. dwc-2: Investigation by Box-Behnken design method, J. Mol. Liq., 221 (2016) 156–165.

[24] H.F. Li, Y.B. Lin, W.M. Guan, J.L. Chang, L. Xu, J.K. Guo, G.H. Wei, Biosorption of Zn (II) by live and dead cells of *Streptomyces ciscaucasicus* strain CCNWHX 72-14, J. Hazard. Mater., 179 (2010) 151–159.

[25] V.S. Munagapati, D. Kim, Equilibrium isotherms, kinetics, and thermodynamics studies for Congo red adsorption using calcium alginate beads impregnated with nano-goethite, Ecotoxicol. Environ. Saf., 141 (2017) 226–234.

[26] I.B. Stephen, J.T. Chien, G.H. Ho, J. Yang, B.H. Chen, Equilibrium and kinetic studies on sorption of basic dyes by a natural biopolymer poly (c-glutamic acid), Biochem. Eng. J., 31 (2006) 204–215.

[27] J.Y. Wang, C.W. Cui, Characterization of the biosorption properties of dormant spores of *Aspergillus niger*: A potential breakthrough agent for removing Cu^{2+} from contaminated water, RSC. Adv., 7 (2017) 14069–14077.

[28] Z.M. Puyen, E. Villagrasa, J. Maldonado, E. Diestra, I. Esteve, A. Solé, Biosorption of lead and copper by heavy-metal tolerant *Micrococcus luteus* DE2008, Bioresour. Technol., 126 (2012) 233–237.

[29] M. Akbari, A. Hallajisani, A.R. Keshtkar, H. Shahbeig, S.A. Ghorbanian, Equilibrium and kinetic study and modeling of Cu (II) and Co (II) synergistic biosorption from Cu (II)-Co (II) single and binary mixtures on brown algae C. indica, J. Environ. Chem. Eng., 3 (2015) 140–149.

[30] T. Kiran, A.S. Akar, A. Ozcan, S. Ozcan Tunali, Biosorption kinetics and isotherm studies of acid red 57 by dried *Cephalosporium aphidicola* cells from aqueous solutions, Biochem. Eng. J., 31 (2006) 197–203.

[31] P.X. Sheng, Y.P. Ting, J.P. Chen, L. Hong, Sorption of lead, copper, cadmium, zinc, and nickel by marine algal biomass: Characterization of biosorption capacity and investigation of mechanism, J. Colloid Interface Sci., 275 (2004) 131–141.

[32] Y.H. Wu, Y.J. Wen, J.X. Zhou, Q. Dai, Y.Y. Wu, The characteristics of waste *Saccharomyces cerevisiae* biosorption of arsenic (III). Environ. Sci. Pollut. Res., 19 (2012) 3371–3379.

[33] M. Petrović, T. Šoštarić, M. Stojanović, J. Petrović, M. Mihajlović, A. Cosović, S. Stanković, Mechanism of adsorption of Cu^{2+} and Zn^{2+} on the corn silk (Zea mays L.), Ecol. Eng., 99 (2017) 83–90.

[34] E.A. Dila, M. Ghaedia, G.R. Ghezelbashb, A. Asfarama, M.K. Purkait, Highly efficient simultaneous biosorption of Hg^{2+}, Pb^{2+} and Cu^{2+} by Live yeast *Yarrowia lipolytica* 70562 following response surface methodology optimization: Kinetic and isotherm study, J. Ind. Eng. Chem., 48 (2017) 162–172.
[35] H.S. Li, Y.H. Chen, J.Y. Long, X.W. Li, D.Q. Jiang, P. Zhang, J.Y. Qi, X.X. Huang, J. Liu, R.B. Xu, J. Gong, Removal of thallium from aqueous solutions using Fe-Mn binary oxides, J. Hazard. Mater., 338 (2017) 296–305.
[36] M.X. Li, H.B. Liu, T.H. Chen, T. Hayat, N.S. Alharbi, C.L. Chen, Adsorption of europium on al-substituted goethite. J. Mol. Liq., 236 (2017) 445–451.
[37] L. Ramrakhiani, R. Majumder, S. Khowala, Removal of hexavalent chromium by heat inactivated fungal biomass of *Termitomyces clypeatus*: Surface characterization and mechanism of biosorption, Chem. Eng. J., 171 (2011) 1060–1068.
[38] F. Huang, Z. Dang, C.L. Guo, G.N. Lu, R.R. Gu, H.J. Liu, H. Zhang, Biosorption of Cd (II) by live and dead cells of Bacillus cereus RC-1 isolated from cadmium-contaminated soil. Colloid Surface 107 (2013) 11–18.
[39] M. Aryal, M. Ziagova, M.L. Kyriakides, Study on arsenic biosorption using Fe (III)-treated biomass of *Staphylococcus xylosus*, Chem. Eng. J., 162 (2010) 178–185.
[40] X.L. Mohamad, P. Hao, S. Xie, Hatab, Y.B. Lin, G.H. Wei, Biosorption of copper (II) from aqueous solution using non-living *Mesorhizobium amorphae* strain CCNWGS0123, Microbes Environ., 27 (2017) 217–225.
[41] K.A. Shroff, V.K. Vaidya, Kinetics and equilibrium studies on biosorption of nickel from aqueous solution by dead fungal biomass of *Mucor hiemalis*, Chem. Eng. J., 171 (2011) 1234–1245.
[42] M. Roushani, Z. Saedi, Y.M. Baghelani, Removal of cadmium ions from aqueous solutions using TMU-16-NH2 metal organic framework, Environ. Nanotechnology, Monit. Manage., 7 (2017) 89–96.
[43] S.Y. Kim, M.R. Jin, C.H. Chung, Y.S. Yun, K.Y. Jahng, K.Y. Yu, Biosorption of cationic basic dye and cadmium by the novel biosorbent *Bacillus catenulatus* JB-022 strain, J. Biosci. Bioeng., 119 (2015) 433–439.
[44] Z.J. Deng, L.X. Cao, H.W. Huang, X.Y. Jiang, W.F. Wang, Y. Shi, R.D. Zhang, Characterization of Cd- and Pb-resistant fungal endophyte Mucor sp. CBRF59 isolated fromrapes (Brassica chinensis) in a metal-contaminated soil, J. Hazard. Mater., 185 (2011) 717–724.
[45] H.S. Li, Y.H. Chen, J.Y. Long, D.Q. Jiang, J. Liu, S.J. Li, J.Y. Qi, P. Zhang, J. Wang, J. Gong, Q.H. Wu, D.Y. Chen, Simultaneous removal of thallium and chloride from a highly saline industrial wastewater using modified anion exchange resins, J. Hazard. Mater., 333 (2017) 179–185.
[46] M.A. Badawi, N.A. Negm, M.T.H. Abou Kana, H.H. Hefni, M.M. Abdel Moneim, Adsorption of aluminum and lead from wastewater by chitosan-tannic acid modified biopolymers: Isotherms, kinetics, thermodynamics and process mechanism, Int. J. Biol. Macromol., 99 (2017) 465–476.
[47] J. Tang, Y. Li, X. Wang, M. Daroch, Effective adsorption of aqueous Pb2t by dried biomass of Landoltia punctata and Spirodela polyrhiza, J. Clean. Prod., 145 (2017) 25–34.
[48] B. Henriques, L.S. Rocha, C.B. Lopes, P. Figueira, R.J.R. Monteiro, A.C. Duarte, M.A. Pardal, E. Pereira, Study on bioaccumulation and biosorption of mercury by living marine macroalgae: Prospecting for a new remediation biotechnology applied to saline waters. Chem. Eng. J., 281 (2015) 759–770.
[49] E. Carlos, C. Flores, L.F.C. Ruiz, M.C.A. Torre, M.A. Huerta-Diaz, J.R. Rangel-Mendez, Biosorption removal of benzene and toluene by three dried macroalgae at different ionic strength and temperatures: Algae biochemical composition and kinetics, J. Environ. Manage., 193 (2017) 126–135.
[50] W.C. Yang, S.Q. Tian, Q.Z. Tang, L.Y. Chai, H.Y. Wang, Fungus hyphae-supported alumina: An efficient and reclaimable adsorbent for fluoride removal from water, J. Colloid Interface Sci., 496 (2017) 496–504.
[51] A. Verma, S. Kumar, S. Kumar, Biosorption of lead ions from the aqueous solution by *Sargassum filipendula*: Equilibrium and kinetic studies, Chem. Eng. J., 4 (2016) 4587–4599.
[52] E. Bagda, T. Mustafa, S. Ahmet, Equilibrium, thermodynamic and kinetic investigations for biosorption of uranium with green algae (*Cladophora hutchinsiae*), J. Environ. Radioactiv., 175–176 (2017) 7–14.
[53] Z.F. Ren, X. Xu, X. Wang, B.Y. Gao, Q.Y. Yue, W. Song, L. Zhang, H.T. Wang, FTIR, Raman, and XPS analysis during phosphate, nitrate and Cr (VI) removal by amine cross-linking biosorbent, J. Colloid Interface Sci., 468 (2016) 313–323.
[54] D. Gola, P. Dey, A. Bhattacharya, A. Mishra, A. Malik, M. Namburath, S.Z. Ahammad, Multiple heavy metal removal using an entomopathogenic fungi *Beauveria bassiana*, Bio. Tech., 218 (2016) 388–396.
[55] Y. Zhou, Z.Q. Zhang, J. Zhang, S.Q. Xia, New insight into adsorption characteristics and mechanisms of the biosorbent from waste activated sludge for heavy metals, J. Environ. Sci., 45 (2016) 248–256.
[56] Y.Y. Qu, H. Li, A. Li, F. Ma, J.T. Zhou, Identification and characterization of Leucobacter sp. N-4 for Ni (II) biosorption by response surface methodology, J. Hazard. Mater., 190 (2017) 869–875.
[57] R.M. Kulkarni, K.V. Shetty, G. Srinikethan, Cadmium (II) and nickel (II) biosorption by *Bacillus laterosporus* (MTCC 1628), J. Taiwan Inst. Chem. Eng., 45 (2014) 1628–1635.
[58] H.G. Zhang, H.S. Li, M. Li, D.G. Luo, Y.H. Chen, D.Y. Chen, H.L. Luo, Z.X. Chen, K.K. Li, Immobilization of metal-resistant sulfate reducing bacteria for cadmium removal from aqueous solutions, Pol. J. Environ. Stud. Accepted.
[59] H. Xu, L. Tan, H.G. Dong, J. He, X.X. Liu, G.Z. Qiu, Q.F. He, J.P. Xie, Competitive biosorption behavior of Pt (IV) and Pd (II) by *Providencia vermicola*, RSC. Adv., 7 (2017) 32229–32235.
[60] P.L. Lalhmunsiama, H. Gupta Jung, D. Tiwari, S.H. Kong, S.M. Lee, Insight into the mechanism of Cd (II) and Pb (II) removal by sustainable magnetic biosorbent precursor to Chlorella vulgaris, J. Taiwan Inst. Chem. Eng., 71 (2017) 206–213.
[61] W. Zhang, L.Y. Meng, G.Q. Mu, M.J. Zhao, P. Zou, Y.S. Zhang, A facile strategy for fabrication of nano-ZnO/yeast composites and their adsorption mechanism towards lead (II) ions, Appl. Surf. Sci., 378 (2016) 196–206.